

New Active Power Filter Topology for Grid Support and Harmonic Mitigation in Interconnecting Renewable Power Generation Systems

Maloth Laxman¹, Nomula Ganesh.²

¹ M.Tech Student

Siddhartha Institute of Technology & Science
Hyderabad, India

² Associate prof, M.Tech

Siddhartha Institute of Technology & Science
Hyderabad, India

Abstract: Renewable generation affects power quality due to its nonlinearity, since solar generation plants and wind power generators must be connected to the grid through high-power static PWM converters. This paper presents active power filter implemented with a four-leg voltage-source inverter. A Novel predictive control scheme is implemented to control the inverter. The main features of this control scheme is 1) To predict the future behavior of the variables to be controlled. The controller uses this information to select the optimum switching state that will be applied to the power converter. 2) To control power converter to inject power generated from RES to the grid, and 2) To act as a shunt APF to compensate current unbalance, load current harmonics, load reactive power demand and load neutral current. The compensation performance of the proposed active power filter and the associated control scheme under steady state and transient operating conditions is demonstrated through simulations results.

Index Terms—Active power filter, current control, four-leg converters, predictive control.

I. INTRODUCTION

Electric utilities and end users of electric power are becoming increasingly concerned about meeting the growing energy demand. Seventy five percent of total global energy demand is supplied by the burning of fossil fuels. But increasing air pollution, global warming concerns, diminishing fossil fuels and their increasing cost have made it necessary to look towards renewable sources as a future energy solution. Since the past decade, there has been an enormous interest in many countries on renewable energy for power generation. The market liberalization and government's incentives have further accelerated the renewable energy sector growth.

Renewable energy source (RES) integrated at distribution level is termed as distributed generation (DG). The utility is concerned due to the high penetration level of intermittent RES in distribution systems as it may pose a threat to network in terms of stability, voltage regulation and power-quality (PQ) issues. Therefore, the DG systems are required to comply with strict technical and regulatory frameworks to ensure safe, reliable and efficient operation of overall network. With the advancement in power electronics and digital control technology, the DG systems can now be actively controlled to enhance the system operation with improved PQ at PCC. However, the extensive use of power electronics based equipment and non-linear loads at PCC generate harmonic currents, which may deteriorate the quality of power [1], [2].

Generally, current controlled voltage source inverters are used to interface the intermittent RES in distributed system.

Recently, a few control strategies for grid connected inverters incorporating PQ solution have been proposed. In [3] an inverter operates as active inductor at a certain frequency to absorb the harmonic current. But the exact calculation of network inductance in real-time is difficult and may deteriorate the control performance. A similar approach in which a shunt active filter acts as active conductance to damp out the harmonics in distribution network is proposed in [4]. In [5], a control strategy for renewable interfacing inverter based on – theory is proposed. In this strategy both load and inverter current sensing is required to compensate the load current harmonics.

The non-linear load current harmonics may result in voltage harmonics and can create a serious PQ problem in the power system network. Active power filters (APF) are extensively used to compensate the load current harmonics and load unbalance at distribution level. This results in an additional hardware cost. However, in this paper authors have incorporated the features of APF in the, conventional inverter interfacing renewable with the grid, without any additional hardware cost. Here, the main idea is the maximum utilization of inverter rating which is most of the time underutilized due to intermittent nature of RES.

This paper presents the mathematical model of the 4L-VSI and the principles of operation of the proposed predictive control scheme, including the design procedure. The complete description of the selected current reference generator implemented in the active power filter is also presented. It is shown in this paper that the grid-interfacing inverter can

effectively be utilized to perform following important functions: 1) transfer of active power harvested from the renewable resources (wind, solar, etc.); 2) load reactive power demand support; 3) current harmonics compensation at PCC; and 4) current unbalance and neutral current compensation in case of 3-phase 4-wire system. Moreover, with adequate control of grid-interfacing inverter, all the four objectives can be accomplished either individually or simultaneously.

II. SYSTEM DESCRIPTION

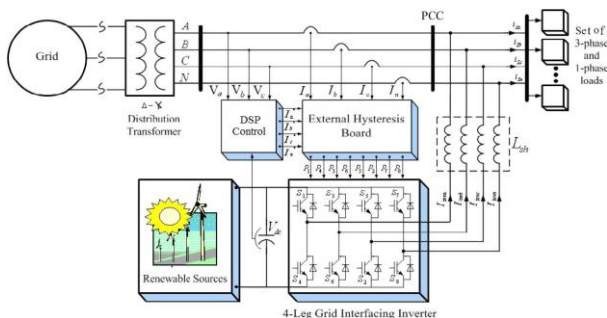


Fig. 1. Schematic of proposed renewable based distributed generation system.

The proposed system consists of RES connected to the dc-link of a grid-interfacing inverter as shown in Fig. 1. The voltage source inverter is a key element of a DG system as it interfaces the renewable energy source to the grid and delivers the generated power. The RES may be a DC source or an AC source with rectifier coupled to dc-link. Usually, the fuel cell and photovoltaic energy sources generate power at variable low dc voltage, while the variable speed wind turbines generate power at variable ac voltage. Thus, the power generated from these renewable sources needs power conditioning (i.e., dc/dc or ac/dc) before connecting on dc-link [6]–[8]. The dc-capacitor decouples the RES from grid and also allows independent control of converters on either side of dc-link.

III. MODELLING OF INVERTER

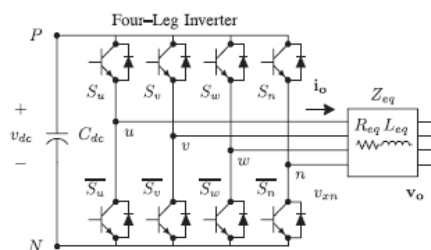


Fig. 2. Two-level four-leg PWM-VSI topology.

NOMENCLATURE

AC	Alternating current.
dc	Direct current.
PWM	Pulse width modulation.
PC	Predictive controller.
PLL	Phase-locked-loop.
V _{dc}	Dc-voltage.
V_s	System voltage vector $[v_{su} \ v_{sv} \ v_{sw}]^T$.
I_s	System current vector $[i_{su} \ i_{sv} \ i_{sw}]^T$.
I_l	Load current vector $[i_{Lu} \ i_{Lv} \ i_{Lw}]^T$.
V_o	VSI output voltage vector $[v_{ou} \ v_{ov} \ v_{ow}]^T$.
I_o	VSI output current vector $[i_{ou} \ i_{ov} \ i_{ow}]^T$ i[*] o
	Reference current vector $[i^{*u} \ i^{*v} \ i^{*w}]^T$.
I _n	Neutral current.
L _f	Filter inductance.
R _f	Filter resistance.

The four-leg PWM converter topology is shown in Fig. 2. This converter topology is similar to the conventional three-phase converter with the fourth leg connected to the neutral bus of the system. The fourth leg increases switching states from 8 (2^3) to 16 (2^4), improving control flexibility and output voltage quality[9], and is suitable for current unbalanced compensation. The voltage in any leg *x* of the converter, measured from the neutral point (*n*), can be expressed in terms of switching states, as follows:

$$v_{xn} = S_x - S_n \text{ vdc, } x = u, v, w, n. \quad (1)$$

The mathematical model of the filter derived from the equivalent circuit

$$v_o = v_{xn} - R_{eq} \mathbf{i}_o - L_{eq} \mathbf{di}_o/dt \quad (2)$$

where R_{eq} and L_{eq} are the 4L-VSI output parameters expressed as Thevenin impedances at the converter output terminals Z_{eq} . Therefore, the Thevenin equivalent impedance is determined by a series connection of the ripple filter impedance Z_f and a parallel arrangement between the system equivalent impedance Z_s and the load impedance Z_L

$$Z_{eq} = Z_s Z_L / (Z_s + Z_L) + Z_f \approx Z_s + Z_f. \quad (3)$$

For this model, it is assumed that $Z_L > Z_s$, that the resistive part of the system's equivalent impedance is neglected, and that the series reactance is in the range of 3–7% p.u., which is an acceptable approximation of the real system. Finally, in (2) $R_{eq} = R_f$ and $L_{eq} = L_s + L_f$.

IV. DIGITAL PREDICTIVE CURRENT CONTROL

The block diagram of the proposed digital predictive current control scheme is shown in Fig. 3. This control scheme is basically an optimization algorithm and, therefore, it has to be implemented in a microprocessor.

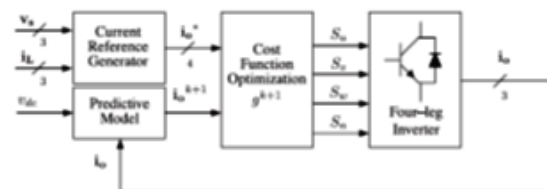


Fig. 3. Proposed predictive digital current control block diagram.

Consequently, the analysis has to be developed using discrete mathematics in order to consider additional restrictions such as time delays and approximations [10], [11]–[17]. The main characteristic of predictive control is the use of the system model to predict the future behavior of the variables to be controlled. The controller uses this information to select the optimum switching state that will be applied to the power converter, according to predefined optimization criteria. The predictive control algorithm is easy to implement and to understand, and it can be implemented with three main blocks, as shown in Fig. 3

1) **Current Reference Generator:** This unit is designed to generate the required current reference that is used to compensate the undesirable load current components. In this case, the system voltages, the load currents, and the dc-voltage converter are measured, while the neutral output current and neutral load current are generated directly from these signals (IV).

2) **Prediction Model:** The converter model is used to predict the output converter current. Since the controller operates in discrete time, both the controller and the system model must be represented in a discrete time domain [11]. The discrete time model consists of a recursive matrix equation that represents

this prediction system. This means that for a given sampling time T_s , knowing the converter switching states and control variables at instant kT_s , it is possible to predict the next states at any instant $[k + 1]T_s$. Due to the first-order nature of the state equations that describe the model in (1)–(2), a sufficiently accurate first-order approximation of the derivative is considered in this paper.

$$dx/dt \approx x[k + 1] - x[k]/T_s \quad (4)$$

The 16 possible output current predicted values can be obtained from (2) and (4) as

$$\mathbf{i}_o[k+1] = T_s / L_{eq} (v_{xn}[k] - \mathbf{v}_o[k]) (1 - (R_{eq} T_s) / L_{eq}) * \mathbf{i}_o[k] \quad (5)$$

As shown in (5), in order to predict the output current \mathbf{i}_o at the instant $(k + 1)$, the input voltage value \mathbf{v}_o and the converter output voltage v_{xN} , are required. The algorithm calculates all 16 values associated with the possible combinations that the state variables can achieve.

3) Cost Function Optimization: In order to select the optimal switching state that must be applied to the power converter, the 16 predicted values obtained for $\mathbf{i}_o[k + 1]$ are compared with the reference using a cost function g , as follows:

$$g[k + 1] = (\mathbf{i}^*_{ou}[k + 1]^2 - \mathbf{i}_{ou}[k + 1]^2) + (\mathbf{i}^*_{ov}[k + 1]^2 - \mathbf{i}_{ov}[k + 1]^2) + (\mathbf{i}^*_{ow}[k + 1]^2 - \mathbf{i}_{ow}[k + 1]^2) + (\mathbf{i}^*_{on}[k + 1]^2 - \mathbf{i}_{on}[k + 1]^2) \quad (6)$$

The output current (\mathbf{i}_o) is equal to the reference (\mathbf{i}^*_{o}) when $g = 0$. Therefore, the optimization goal of the cost function is to achieve a g value close to zero. The voltage vector \mathbf{v}_xN that minimizes the cost function is chosen and then applied at the next sampling state. During each sampling state, the switching state that generates the minimum value of g is selected from the 16 possible function values. The algorithm selects the switching state that produces this minimal value and applies it to the converter during the $k + 1$ state.

V. SYNCHRONOUS REFERENCE THEORY (SRF) FOR CURRENT REFERENCE GENERATION

In the SRF, the load current signals are transformed into the conventional rotating frame d-q. If θ is the transformation angle, The transformation is defined by:

$$\begin{bmatrix} x_d \\ x_q \\ x_0 \end{bmatrix} = \frac{2}{3} \begin{bmatrix} \cos(\theta) & \cos(\theta - \frac{2\pi}{3}) & \cos(\theta - \frac{4\pi}{3}) \\ -\sin(\theta) & \sin(\theta - \frac{2\pi}{3}) & -\sin(\theta - \frac{4\pi}{3}) \\ \frac{1}{\sqrt{2}} & \frac{1}{\sqrt{2}} & \frac{1}{\sqrt{2}} \end{bmatrix} \begin{bmatrix} x_a \\ x_b \\ x_c \end{bmatrix} \quad (7)$$

Where x denotes voltages or currents.

In the SRF θ is a time varying angle that represents the angular position of the reference frame which is rotating at constant speed in synchronism with the three phase ac voltages. To implement the SRF method some kind of synchronizing system should be used. In phase-locked loop (PLL) is used for the implementation of this method. In this case the speed of the reference frame is practically constant, that is, the method behaves as if the reference frame's moment of inertia is infinite. The fundamental currents of the d-q components are now dc values

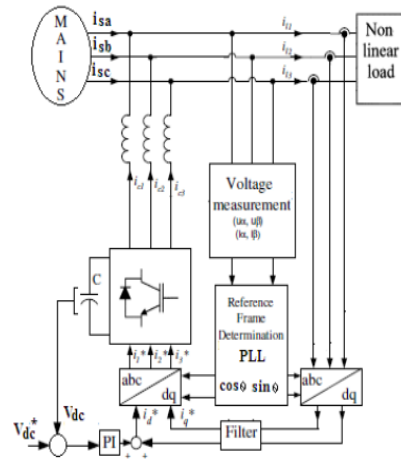


Fig. 4: Basic Synchronous Reference Frame Configuration

The harmonics appear like ripple. Harmonic isolation of the d-q transformed signal is achieved by removing the dc offset. This is accomplished using high pass filters (HPF). In spite of a high pass filter, a low pass filter is used to obtain the reference source current in d-q coordinates. Fig 4 illustrates a configuration of the SRF method. There is no need to supply voltage waveform for a SRF based controller. However the phase position angle must be determined using voltage information. The SRF harmonic detection method can be reasonably summarized as a block diagram as shown in Fig.5.

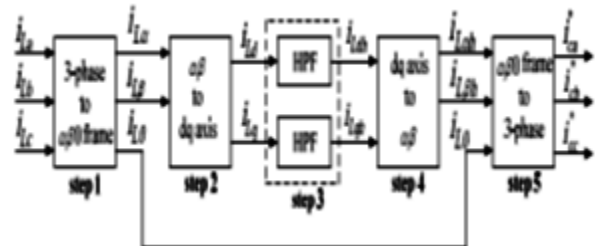


Fig.5: SRF harmonic detection

The current that flows through the neutral of the load is compensated by injecting the same instantaneous value obtained from the phase-currents, phase-shifted by 180°, as shown next

$$\mathbf{i}^*_{on} = -(\mathbf{i}_L u + \mathbf{i}_L v + \mathbf{i}_L w) \quad (8)$$

VI. DC-LINK VOLTAGE AND POWER CONTROL OPERATION

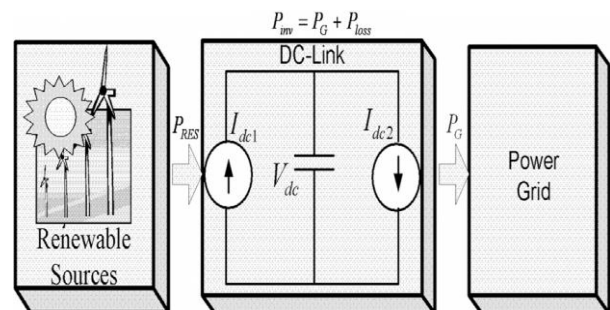


Fig. 6: DC-Link equivalent diagram.

Due to the intermittent nature of RES, the generated power is of variable nature. The dc-link plays an important role in transferring this variable power from renewable energy source to the grid. RES are represented as current sources connected to the dc-link of a grid-interfacing inverter. Fig. 6 shows the systematic representation of power transfer from the renewable energy resources to the grid via the dc-link. The current injected by renewable into dc-link at voltage level can be given as

$$I_{dc1} = P_{res} / V_{dc} \quad (9)$$

where P_{res} is the power generated from RES. The current flow on the other side of dc-link can be represented as,

$$I_{dc2} = P_{inv} / V_{dc} = P_G + P_{LOSS} \quad (10)$$

Where P_{inv} , P_G and P_{LOSS} are total power available at grid-interfacing inverter side, active power supplied to the grid and inverter losses, respectively. If inverter losses are negligible then

$$P_{res} = P_G \quad (11)$$

V. SIMULATED RESULTS

A simulation model for the three-phase four-leg PWM converter has been developed using MATLAB-Simulink. The objective is to verify the current harmonic compensation effectiveness of the proposed control scheme under different operating conditions. A six-pulse rectifier was used as a nonlinear load. The proposed predictive control algorithm was programmed using an S-function block that allows simulation of a discrete model. Simulations were performed considering a 20 [μs] of sample time. In the simulated results shown in Fig. 8, the active filter starts to compensate at $t = t1$. At this time, the active power filter injects an output current i_{ou} to compensate current harmonic components, current unbalanced, and neutral current simultaneously. During compensation, the system currents i_s show sinusoidal waveform, with low total harmonic distortion (THD = 3.93%).

At $t = t2$, a three-phase balanced load step change is generated from 0.6 to 1.0 p.u. The compensated system currents remain sinusoidal despite the change in the load current magnitude. Finally, at $t = t3$, a single-phase load step change is introduced in phase u from 1.0 to 1.3 p.u., which is equivalent to an 11% current imbalance. As expected on the load side, a neutral current flows through the neutral conductor (i_{Ln}), but on the source side, no neutral current is observed (i_{sn}). Simulated results show that the proposed control scheme effectively eliminates unbalanced currents. Additionally, Fig. 8 shows that the dc-voltage remains stable throughout the whole active power filter operation.

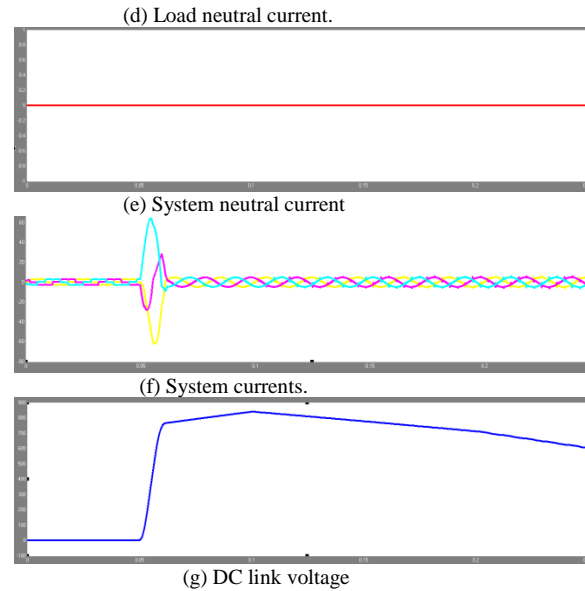
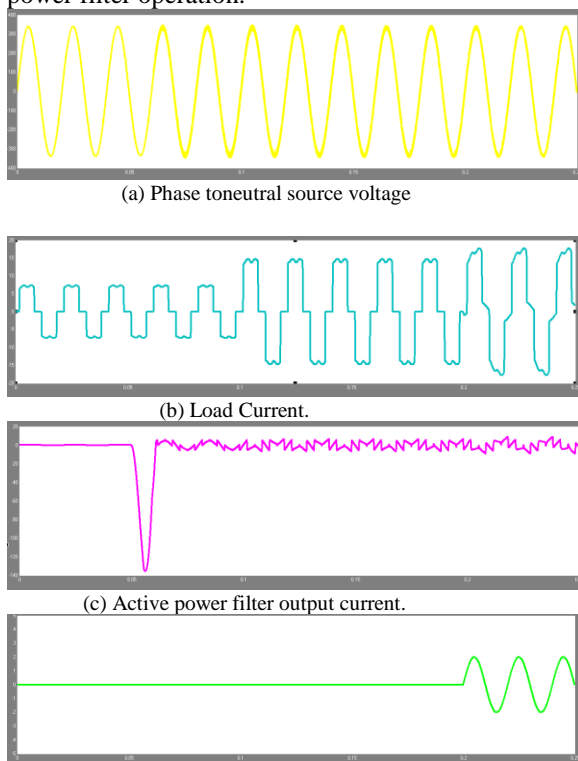


Fig. 7. Simulated waveforms of the proposed control scheme

At $t = 0.72$ s, the inverter starts injecting active power generated from RES ($P_{RES} = P_{inv}$). Since the generated power is more than the load power demand the additional power is fed back to the grid. The negative sign of P_{Grid} , after time 0.72 s suggests that the grid is now receiving power from RES. Moreover, the grid-interfacing inverter also supplies the load reactive power demand locally. Thus, once the inverter is in operation the grid only supplies/receives fundamental active power.

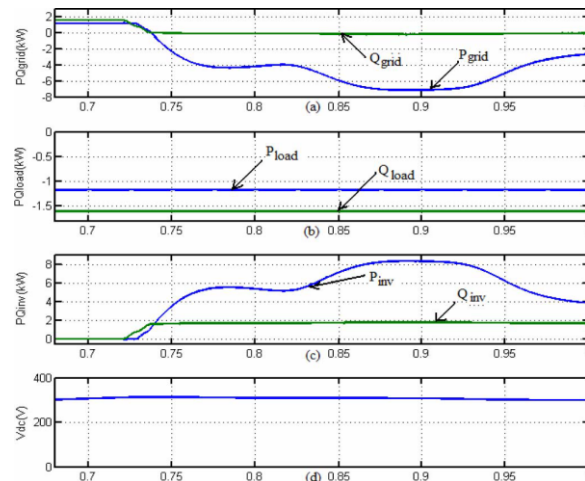


Fig. 8. Simulation results: (a) PQ-Grid, (b) PQ-Load, (c) PQ-Inverter, (d) dc-link voltage.

At $t = 0.82$ s, the active power from RES is increased to evaluate the performance of system under variable power generation from RES. This results in increased magnitude of inverter current. As the load power demand is considered as constant, this additional power generated from RES flows towards grid, which can be noticed from the increased magnitude of grid current as indicated by its profile.

At $t = 0.92$ s, the power available from RES is reduced. The corresponding change in the inverter and grid currents can be seen from Fig. 4. The active and reactive power flows between the inverter, load and grid during increase and decrease of energy generation from RES can be noticed from Fig. 8. The dc-link voltage across the grid-interfacing inverter (Fig. 8(d)) during different operating condition is maintained at constant level in order to facilitate the active and reactive power flow. Thus from the simulation results, it is evident that the grid-interfacing inverter can be effectively used to compensate the load reactive power, current unbalance and current harmonics in addition to active power injection from RES. This enables

the grid to supply/ receive sinusoidal and balanced power at UPF.

VI. CONCLUSION

This paper has presented a novel control of an existing grid interfacing inverter to improve the quality of power at PCC for a 3-phase 4-wire DG system. It has been shown that the grid-interfacing inverter can be effectively utilized for power conditioning without affecting its normal operation of real power transfer. The grid-interfacing inverter with the proposed approach can be utilized to i) Inject real power generated from RES to the grid, and/or, ii) operates as a shunt Active Power Filter (APF). iii) The use of a predictive control algorithm for the converter current loop proved to be an effective solution for active power filter applications, improving current tracking capability, and transient response. Simulated and experimental results have proved that the proposed predictive control algorithm is a good alternative to classical linear control methods. The predictive current control algorithm is a stable and robust solution. Simulated and experimental results have shown the compensation effectiveness of the proposed active power filter.

VII. REFERENCES

[1] J. Rocabert, A. Luna, F. Blaabjerg, and P. Rodriguez, "Control of power converters in AC microgrids," *IEEE Trans. Power Electron.*, vol. 27, no. 11, pp. 4734–4749, Nov. 2012.

[2] M. Aredes, J. Hafner, and K. Heumann, "Three-phase four-wire shunt active filter control strategies," *IEEE Trans. Power Electron.*, vol. 12, no. 2, pp. 311–318, Mar. 1997.

[3] S. Naidu and D. Fernandes, "Dynamic voltage restorer based on a fourleg voltage source converter," *Gener. Transm. Distrib., IET*, vol. 3, no. 5, pp. 437–447, May 2009.

[4] N. Prabhakar and M. Mishra, "Dynamic hysteresis current control to minimize switching for three-phase four-leg VSI topology to compensate nonlinear load," *IEEE Trans. Power Electron.*, vol. 25, no. 8, pp. 1935–1942, Aug. 2010.

[5] V. Khadkikar, A. Chandra, and B. Singh, "Digital signal processor implementation and performance evaluation of split capacitor, four-leg and three h-bridge-based three-phase four-wire shunt active filters," *PowerElectron., IET*, vol. 4, no. 4, pp. 463–470, Apr. 2011.

[6] F. Blaabjerg, R. Teodorescu, M. Liserre, and A. V. Timbus, "Overview of control and grid synchronization for distributed power generation systems," *IEEE Trans. Ind. Electron.*, vol. 53, no. 5, pp. 1398–1409, Oct. 2006.

[7] J. M. Carrasco, L. G. Franquelo, J. T. Bialasiewicz, E. Galván, R. C. P. Guisado, M. Á. M. Prats, J. I. León, and N. M. Alfonso, "Power electronic systems for the grid integration of renewable energy sources: A survey," *IEEE Trans. Ind. Electron.*, vol. 53, no. 4, pp. 1002–1016, Aug. 2006.

[8] B. Renders, K. De Gussemme, W. R. Ryckaert, K. Stockman, L. Vandeveld, and M. H. J. Bollen, "Distributed generation for mitigating voltage dips in low-voltage distribution grids," *IEEE Trans. Power. Del.*, vol. 23, no. 3, pp. 1581–1588, Jul. 2008.

[9] S. Ali, M. Kazmierkowski, "PWM voltage and current control of four-leg VSI," presented at the ISIE, Pretoria, South Africa, vol. 1, pp. 196–201, Jul. 1998

[10] P. Cortes, G. Ortiz, J. Yuz, J. Rodriguez, S. Vazquez, and L. Franquelo, "Model predictive control of an inverter with output LC filter for UPS applications," *IEEE Trans. Ind. Electron.*, vol. 56, no. 6, pp. 1875–1883, Jun. 2009.

[12] S. Kouro, P. Cortes, R. Vargas, U. Ammann, and J. Rodriguez, "Model predictive control—A simple and powerful method to control power converters," *IEEE Trans. Ind. Electron.*, vol. 56, no. 6, pp. 1826–1838, Jun. 2009.

[13] D. Quevedo, R. Aguilera, M. Perez, P. Cortes, and R. Lizana, "Model predictive control of an AFE rectifier with dynamic references," *IEEE Trans. Power Electron.*, vol. 27, no. 7, pp. 3128–3136, Jul. 2012.

[14] Z. Shen, X. Chang, W. Wang, X. Tan, N. Yan, and H. Min, "Predictive digital current control of single-inductor multiple-output converters in CCM with low cross regulation," *IEEE Trans. Power Electron.*, vol. 27, no. 4, pp. 1917–1925, Apr. 2012.

[15] M. Rivera, C. Rojas, J. Rodriguez, P. Wheeler, B. Wu, and J. Espinoza, "Predictive current control with input filter resonance mitigation for a direct matrix converter," *IEEE Trans. Power Electron.*, vol. 26, no. 10, pp. 2794–2803, Oct. 2011.

[16] M. Preindl and S. Bolognani, "Model predictive direct speed control with finite control set of PMSM drive systems," *IEEE Trans. Power Electron.*, 2012.

[17] T. GEYER, "COMPUTATIONALLY EFFICIENT MODEL PREDICTIVE DIRECT TORQUE CONTROL," *IEEE TRANS. POWER ELECTRON.*, VOL. 26, NO. 10, PP. 2